

Particle-hole state densities with non-equidistant single-particle levels

A. Harangozo, I. Şteţcu, M. Avrigeanu, and V. Avrigeanu

Institute for Nuclear Physics and Engineering, P.O. Box MG-6, 76900 Bucharest, Romania

submitted for publication in Phys. Rev. C

Abstract

The correct use of energy-dependent single-particle level (s.p.l.) densities within particle-hole state densities based on the equidistant spacing model (ESM) is analysed. First, an analytical expression is obtained following the convolution of energy-dependent excited-particle and hole densities. Next, a comparison is made with results of the ESM formula using average s.p.l. densities for the excited particles and holes, respectively. The Fermi-gas model (FGM) s.p.l. densities calculated at the corresponding average excitation energies are used in both cases. The analysis concerns also the density of particle-hole bound states. The pairing correlations are taken into account while the comparison of various effects includes the exact correction for the Pauli exclusion principle. Quantum-mechanical s.p.l. densities and the *continuum effect* can also match a corresponding FGM formula, suitable for use within the average energy-dependent partial state density in multistep reaction models.

PACS: 21.10.Ma, 21.10.Pc, 24.60.Dr, 24.60.Gv

Typeset using REVTeX

I. INTRODUCTION

The particle-hole state densities are basic quantities for the description of preequilibrium emission (PE) in semiclassical models as well as quantum-statistical theories (e.g., [1,2]) involving a series of particle-hole excitations caused by two-body interactions. The nuclear excitation in the equilibrium processes concerns the single-particle levels (s.p.l.) within an energy range of the order of the nuclear temperature around the Fermi level. This explains the basic role of the s.p.l. equidistant spacing model (ESM) [3] in the analysis of the equilibrium emission (see also [4]). However, much higher and lower single-particle energies are involved in PE reactions so that one should consider the reduced suitability of the ESM partial-state density (PSD) formula of Williams [5]. Moreover, the inconsistency between the phenomenological s.p.l. density $g \sim A/14 \text{ MeV}^{-1}$ and the number A of nucleons in the nucleus has come under increasing criticism [6,7]. On the other hand, combinatorial calculations performed in the space of realistic shell model s.p.l. [8] have other inherent shortcomings (e.g., the strong dependence on the basic set of s.p.l.) [9,10]. This accounts for the continued use of the Williams-type formula with various corrections [11,12] or exact calculation [13] for additional Pauli blocking and the pairing interaction.

In fact, there have been early attempts at considering the single-particle energy dependence of the s.p.l. density $g(\varepsilon)$ within PE formalisms [14–16]. Next, Kalbach [17,18] discussed different forms of this dependence and found it tied to PE surface effects due to the interdependence of the respective assumptions. Herman *et al.* [6] obtained an indication for the energy dependence nearly as that given by the Fermi-gas model (FGM) below the Fermi energy F , but linear above F . Chadwick and Reffo [7] found the use of either the FGM prescription or the equidistant parametrization $g=A/F$ more accurate than the phenomenological one. The FGM s.p.l. density has also been involved in the development of the partial level densities with linear momentum [19]. At the same time, the ESM accuracy has been discussed in connection with the non-uniform s.p.l. density effect [20] provided by the harmonic oscillator model. The analysis of the energy-dependent s.p.l. density in the

vicinity of the Fermi energy [21] provided a more general form and a good approximation of the effect for low energies, where the influence of the finite depth of the potential well can be neglected. Various $g(\varepsilon)$ have been obtained within both the semiclassical Thomas-Fermi approximation [21–28] and the exact quantum mechanical calculations [29–31] which are also applicable at the high excitations located in the continuum region. The PSD including distinct energy-dependences for the excited-particle and hole level densities has recently been used in semiclassical [32] or quantum-statistical [33,34] cross-section calculations.

The valid use of energy-dependent s.p.l. densities within the ESM particle-hole state density formula, even when corrected for the finite depth of the real nuclear potential well [35], has not yet been proved. Proving it is one aim of this work. First, the particle-hole state density is obtained in Sec. II by means of recursive relations particularly using the FGM s.p.l. density. Next, these are compared in Sec. III with the results of the ESM formula modified by using s.p.l. densities different for excited particles and holes, obtained from the FGM at the respective average-excitation energies [18] (the average energy-dependent ESM formalism). The analysis is also carried out for the density of particle-hole bound states, with single-particle excitations not exceeding the nucleon binding energy [36]. The advanced pairing correction [11,12] is taken into account while the comparison of various effects includes the exact correction for the Pauli exclusion principle [13]. The importance of distinct corrections in the average energy-dependent ESM formalism is further discussed in Sec. IV. At the same time the subtraction of the free-gas contribution [29,30,37] is analysed within this formalism, thus making no use of arbitrary truncation [38]. The respective results are compared with the semiclassical and quantum-mechanical calculations of the continuum effect. Since the actual quantum-statistical analyses of the multistep reactions still involve the rough ESM, the respective results could be altered following consideration of the effective NN -interaction strength as the only free parameter. The conclusions are drawn in Sec. V.

II. THE *PSD* RECURSIVE FORMULA

A. Single-particle level densities

Densities of the excited particles and holes with distinct energy dependences or even different values at the Fermi energy F were considered by Gadioli and co-workers [15,16], Běťák and Dobeš [35], and Herman *et al.* [39]. The subsequent study [6] of unperturbed shell-model Hamiltonian spacings indicated a linear energy dependence for excited particles, as well as different corresponding values at the Fermi level. On the other hand, Schmidt *et al.* [40] found that the smooth s.p.l. density in a Woods-Saxon potential lies between the density corresponding to an infinite box and the one for an harmonic oscillator, and approximately follows $g(\varepsilon) \sim \varepsilon$. Moreover, this energy dependence has already been used within an improved abrasion model for heavy-ion collisions [41].

Given the need for an analytical PLD expression, we have followed the method of Bogila *et al.* [21] while the finite depth of the nuclear potential well and the case of particle-hole bound states have also been considered. Actually, the particle-hole bound state formula turns into the common form in the limit of large values of the nucleon binding energy B . The following discussion will concern the general form of $g(\varepsilon)$, with the g_0 value at the Fermi level. However, the usual FGM energy dependence

$$g(\varepsilon) = g_0 \left(\frac{\varepsilon}{F} \right)^{1/2} = \frac{3A}{2F} \left(\frac{\varepsilon}{F} \right)^{1/2} \quad (1)$$

is particularly taken into account (see also the Appendix). This can be expressed in terms of the single-particle excitation energies $u = \varepsilon - F$ for particles, and $u = F - \varepsilon$ for holes. Next, similarly to Bogila *et al.* we have retained the first three terms of its expansion in powers of u around the value at zero excitation energy. The general forms of the excitation-energy dependence then become

$$g_p(u) = (au^2 + bu + c)\theta(B - u) \quad (2)$$

and

$$g_h(u) = (au^2 - bu + c)\theta(F - u), \quad (3)$$

where the theta functions are unity if their argument is greater than zero, and zero otherwise. The FGM values of the coefficients are $a = g_0''/2 = -g_0/8F^2$, $b = g_0' = g_0/2F$, and $c = g_0$, where g_0' and g_0'' are the values at the Fermi level of the respective derivatives. Various energy dependences of the s.p.l. density can obviously be involved within this framework, by using the appropriate values for the coefficients in Eqs. (2-3).

B. The convolution state-density formula

The bound-state density $\omega(p, h, E)$ for p excited particles above the Fermi level and h holes below it ($n = p + h$), at the total excitation energy E , can be obtained by convolution of the single-particle and hole level densities with an excitation-energy conserving delta function [2,7,15]

$$\begin{aligned} \omega(p, h, E) = & \frac{1}{p!h!} \int_0^\infty du_1 g_p(u_1) \int_0^\infty du_2 g_p(u_2) \dots \int_0^\infty du_p g_p(u_p) \\ & \times \int_0^\infty du_1 g_h(u_1) \dots \int_0^\infty du_h g_h(u_h) \delta \left(E - \sum_{\lambda=1}^p u_\lambda - \sum_{j=1}^h u_j \right), \end{aligned} \quad (4)$$

where the Pauli principle is not yet taken into account. One way to proceed [2] is to replace the δ function by its integral representation

$$\delta \left(E - \sum_{\lambda=1}^p u_\lambda - \sum_{j=1}^h u_j \right) = \frac{1}{2\pi} \int_{-\infty}^\infty \exp \left[ik \left(E - \sum_{\lambda=1}^p u_\lambda - \sum_{j=1}^h u_j \right) \right] dk, \quad (5)$$

so that

$$\omega(p, h, E) = \frac{1}{2\pi p!h!} \int_{-\infty}^\infty e^{ikE} \left(\int_0^\infty g_p(u) e^{-iku} du \right)^p \left(\int_0^\infty g_h(u) e^{-iku} du \right)^h dk. \quad (6)$$

By using the s.p.l. densities given by Eqs. (2-3), evaluation of the integrals, and expansion of the respective results, it results

$$\omega(p, h, E) = \frac{g_0^n}{2\pi p!h!} \sum_{\lambda=0}^p \sum_{j=0}^h (-1)^{\lambda+j} C_p^\lambda C_h^j R_{\lambda j} \left(\int_{-\infty}^\infty \frac{\exp[ik(E - \lambda B - jF)]}{(ik)^N} dk \right), \quad (7)$$

where, by replacing λ by i ,

$$\begin{aligned}
R_{ij}(z) &= \sum_{k_1=0}^{p-i} \sum_{i_1=0}^{k_1} \sum_{l_1=0}^{h-j} \sum_{j_1=0}^{l_1} (-1)^{j_1+l_1} C_p^{k_1} C_{k_1}^{i_1} C_{h-j}^{l_1} C_{l_1}^{j_1} \left(\frac{g_0''}{g_0'}\right)^{i_1+j_1} \left(\frac{g_0'}{g_0}\right)^{k_1+l_1} \\
&\quad \times \sum_{k_2=0}^i \sum_{i_2=0}^{k_2} \sum_{l_2=0}^j \sum_{j_2=0}^{l_2} C_i^{k_2} C_{k_2}^{i_2} C_j^{l_2} C_{l_2}^{j_2} \frac{(g_0'')^{i_2+j_2}}{(g_0)^{i+j}} \\
&\quad \times \left(g_0'' \frac{B^2}{2} + g_0' B + g_0\right)^{i-k_2} (g_0'' B + g_0')^{k_2-i_2} \left(g_0'' \frac{F^2}{2} - g_0' F + g_0\right)^{j-l_2} (g_0'' F - g_0')^{l_2-j_2} z, \quad (8a)
\end{aligned}$$

z is the integral which forms the functional argument in Eq. (7), and

$$N = n + i_1 + j_1 + k_1 + l_1 + i_2 + j_2 + k_2 + l_2. \quad (8b)$$

Finally, by using the Cauchy residue theorem we have obtained the expression

$$\begin{aligned}
\omega(p, h, E) &= \frac{g_0^n}{p!h!(n-1)!} \sum_{i=0}^p \sum_{j=0}^h (-1)^{i+j} C_p^i C_h^j (E - iB - jF)^{n-1} \theta(E - iB - jF) \\
&\quad \times R_{ij} \left((E - iB - jF)^{N-n} \frac{(n-1)!}{(N-1)!} \right). \quad (9)
\end{aligned}$$

The $(n-1)$ factorial and power have additionally been included in order to obtain a form similar to those obtained by Obložinský [36] in the frame of the ESM, and Bogila *et al.* [21] within the FGM with no constraints for particles or holes. Thus, in the limiting case of large B and F in the above expression, the i and j indices become zero so that the last four sums in R_{ij} disappear and the formula of Bogila *et al.* is obtained

$$\begin{aligned}
\omega(p, h, E) &= \omega^{\text{E}}(p, h, E) \sum_{k_1=0}^p \sum_{i_1=0}^{k_1} \sum_{l_1=0}^h \sum_{j_1=0}^{l_1} (-1)^{j_1+l_1} C_p^{k_1} C_{k_1}^{i_1} C_h^{l_1} C_{l_1}^{j_1} \\
&\quad \times \left(\frac{g_0''}{g_0'}\right)^{i_1+j_1} \left(\frac{g_0'}{g_0}\right)^{k_1+l_1} E^{i_1+j_1+k_1+l_1} \frac{(n-1)!}{(n-1+i_1+j_1+k_1+l_1)!}, \quad (10)
\end{aligned}$$

where

$$\omega^{\text{E}}(p, h, E) = \frac{g_0^n E^{n-1}}{p!h!(n-1)!} \quad (11)$$

is the well-known Ericson formula [3] for the ESM case. However, we underline that a definite single-particle ground state should be marked out by the finite value of F within a consistent energy-dependent s.p.l. density. Therefore, the finite depth of the nuclear-potential well should be explicitly present in the particle-hole state density formulas exceeding the ESM framework. The usual formula for the density of the particle-hole bound states within the ESM approximation results immediately from Eq. (9) by noting the unity values of all functionals R_{ij} for a constant s.p.l. density. The only difference with respect to the formula of Obložinský [36] concerns the Pauli-blocking factor A_{ph} and the corresponding minimum energy α_{ph} for a p - h state, which have not yet been included here. On the other hand, the temporary omission of the Pauli-principle correction can be used to estimate the energy-dependence effect better. Thus, the ratio between the results of Eq. (9) and Obložinský formula without the Pauli correction is shown in Fig. 1 for a few simple p - h configurations. Here the bound-state condition is released, $g_0=14 \text{ MeV}^{-1}$, and $F=38 \text{ MeV}$. These particle-hole states are actually the most important ones for the PE description, and are least affected by the Pauli-principle oversight. Also shown is the ratio of the PSDs given by Eq. (9) and the Ericson formula, in agreement with the trend of the Bogila *et al.* results (Fig. 1 of Ref. [21]) if one takes into account the different F values used in these analyses. While the former ratio describes the energy-dependence effect versus an ESM formula including the potential finite-depth, the latter has the same role versus the simplest ESM expression of Ericson.

First, the case of the $1p1h$ configuration, Fig. 1(a), shows that the deviation of $g_h(u)$ from g_0 is not really compensated by the corresponding deviation of $g_p(u)$, within the s.p.l. density convolution. Thus, the Obložinský and Ericson formulas provide the same PSD at excitation energies below F , which are higher than the results of Eq. (9). Second, a consideration of the potential finite depth decreases the Obložinský PSD values versus the Ericson formula. At the same time, the results of Eq. (9) decrease less significantly above $E=F$ because of the deviation of $g_p(u)$ from g_0 . Moreover, the case of the $2p1h$ configuration shows the increased importance of the energy dependence versus the Obložinský formula, with the deviation from unity of the respective ratio becoming relevant at excitations higher

than F . Smaller deviations have been obtained [21] as compared with the Ericson expression.

C. Inclusion of Pauli blocking and pairing correction

Following the related forms of the recursive PSD expression (9) and Obložinský formula [36], the correction for the Pauli blocking and pairing effects can be implemented within the former by inclusion of (i) a p - h configuration-dependent threshold energy in the theta function, and (ii) the Pauli-blocking and pairing-correction term of the excitation energy, within the Kalbach formulation [12]

$$A_K(p, h) = E_{\text{th}}(p, h) - \frac{p(p+1) + h(h+1)}{4g_0} + \frac{(p-1)^2 + (h-1)^2}{g_0 F(p, h)}, \quad (12)$$

where the threshold energy

$$E_{\text{th}}(p, h) = \frac{g_0(\Delta_0^2 - \Delta^2)}{4} + p_m \left[\left(\frac{p_m}{g_0} \right)^2 + \Delta^2 \right]^{1/2} \quad (13)$$

is determined by the ground and excited-state gaps Δ_0 and $\Delta(p, h, E)$. The ground-state gap is related to the condensation energy $C = g_0\Delta_0^2/4$ which can be given by the constant-pairing correction U_p [11], based on the odd-even mass differences (e.g., [42]). Δ is obtained by using the parametrization [11,12]

$$\frac{\Delta}{\Delta_0} = [0.996 - 1.76(n/n_c)^{1.60}(E/C)^{-0.68}] \theta(E - E_{\text{phase}}), \quad (14)$$

where $n_c = 0.792g_0\Delta_0$ is the critical number of excitons, and E_{phase} is the energy of the pairing phase transition given by

$$E_{\text{phase}} = C [0.716 + 2.44(n/n_c)^{2.17}] \theta(n/n_c - 0.446). \quad (15)$$

Actually, the latter theta function has been introduced by Kalbach [12] in order to explicitly take into account the lack of a phase transition for small n .

The inclusion of $p_m = \text{maximum}(p, h)$ and the form of the second term in the Kalbach correction (12) have been adopted for a Pauli-correction function symmetric in particles and

holes, including the effects of passive holes. Next, the third term in Eq. (12) has been added in order to force the PSD to have the values of g_0 and $2g_0$ for $E = E_{\text{th}}(p, h)$ and $E = E_{\text{th}}(p, h) + 1/g_0$, respectively. The function

$$F(p, h) = 12 + 4g_0[E - E_{\text{th}}(p, h)]/p_m \quad (16)$$

restricts the action of this third term to just around $E_{\text{th}}(p, h)$.

Consequently, the PSD recursive formula (9), now including the Pauli and pairing corrections, becomes

$$\begin{aligned} \omega(p, h, E) = & \frac{g_0^n}{p!h!(n-1)!} \sum_{i=0}^p \sum_{j=0}^h (-1)^{i+j} C_p^i C_h^j [E - A_K(p, h) - iB - jF]^{n-1} \\ & \times \theta(E - E_{\text{th}} - iB - jF) R_{ij} \left([E - A_K(p, h) - iB - jF]^{N-n} \frac{(n-1)!}{(N-1)!} \right). \end{aligned} \quad (17)$$

The completeness of the Eqs. (9) or (17) has the drawback of making them difficult to use in reaction calculations, due to the intricate form (8a) of the functionals R_{ij} .

III. THE AVERAGE ENERGY-DEPENDENT FORMULA

Since approximate but simpler solutions are still of real interest, we will discuss below the Kalbach [18] attempt to use the energy-dependent s.p.l. density within the ESM formula. In fact, we will be checking its correctness against the exact expression (17). It seems important to note that the Kalbach approach involves distinct but average s.p.l. densities for the holes and excited particles, respectively, at average excitation energies.

A. The finite-depth and pairing corrections

The general form of the ESM density of particle-hole bound states corrected for (i) the Pauli exclusion principle [5], (ii) pairing interactions [11,12], and (iii) the finite depth of the nuclear potential well [35,36] can be written, similarly to Kalbach [18],

$$\omega(p, h, E) = \frac{g_0^n E^{n-1}}{p!h!(n-1)!} f_K(p, h, E, F), \quad (18)$$

where

$$f_K(p, h, E, F) = \sum_{i=0}^p \sum_{j=0}^h (-1)^{i+j} C_p^i C_h^j \left[\frac{E - A_K(p, h) - iB - jF}{E} \right]^{n-1} \times \theta(E - E_{\text{th}} - iB - jF) \quad (19)$$

is a function including the finite-depth, Pauli-blocking and pairing corrections, as well as the bound-state condition. The original correction function [18] was used to modify the PSD formula for the infinite potential well, with the Pauli correction terms $A(p, h)$ neglected in all terms except the leading one. However, by means of Eq. (18) the function $f_K(p, h, E, F)$ can now be regarded as the ratio between the actual PSD formula and the Ericson expression. The index K is related to the inclusion of the advanced pairing correction of Kalbach [12], i.e., of the terms $A_K(p, h)$ and E_{th} .

The importance of the Pauli-blocking and pairing correction term $A_K(p, h)$ is shown in Fig. 2 for simple p - h configurations. First, omission of this correction provides the unit value of the function f_K in the case of the $xp1h$ configurations at excitation energies lower than F . Second, there is a rather similar case (or even identical for the state $1p1h$) if the Pauli correction A_{ph} and the corresponding minimum energy α_{ph} [36] are taken into account but not the pairing corrections. A small threshold behavior becomes apparent in this case. Third, the inclusion of the advanced pairing correction yields a strong reduction at lower excitation energies. Finally, the bound-state condition obviously provides a different function, mainly determined by the number of holes.

B. Single-particle average excitation energies

In order to take into account the long-range deviations from ESM, Kalbach [18] proposed the use of average values for the FGM s.p.l. density (1) corresponding to average excitation energies for either particles or holes. As a first approximation, these energies were estimated in the ESM frame. We follow the same method below but also include the case of the bound states.

The probability for the occurrence of a p - h state with the excitation energy E and an excited particle between u and $u+du$ is given by $g_p(F+u) \cdot \omega(p-1, h, E-u, F) du / \omega(p, h, E, F)$. Consequently, the average excitation energy per excited particle is given by

$$\bar{u}_p = \frac{1}{p} \int_0^{\tilde{B}} \frac{u \cdot g_p(F+u) \omega(p-1, h, E-u, F)}{\omega(p, h, E, F)} du, \quad (20)$$

where $\tilde{B} = \text{minimum}(E, B)$. Assuming a slow energy dependence of the correction term A_K , the average excitation energies for either particles or holes become

$$\bar{u}_p = \frac{E f_K^+(p, h, E, F)}{n f_K(p, h, E, F)} \quad (21a)$$

$$\bar{u}_h = \frac{E - p\bar{u}_p}{h}, \quad (21b)$$

where

$$f_K^+(p, h, E, F) = \sum_{i=0}^p \sum_{j=0}^h (-1)^{i+j} C_p^i C_h^j \left[\frac{E - A_K(p, h) - iB - jF}{E} \right]^n \times \left[1 + \frac{n}{p} \frac{iB}{E - A_K(p, h) - iB - jF} \right] \theta(E - E_{\text{th}} - iB - jF) \quad (22)$$

returns to $f_K(p+1, h, E, F)$ for large B [18]. The shapes of the two functions $f_K(p, h, E, F)$ and $f_K^+(p, h, E, F)$, and the average excitation energies for simple p - h configurations are shown, bound-state case included, in Fig. 3. The above-mentioned similarity between the functions $f_K^+(p, h, E, F)$ and $f_K(p+1, h, E, F)$ can be observed, in the general case, for the $1p1h$ and $2p2h$ -states in Figs. 3(a) and 3(b).

It is worth noting the results of Eqs. (21) for the bound-plus-continuum states shown in Fig. 3(e), and the bound states only as displayed in Fig. 3(f). The distinct trends are due to the separate constraints on hole excitation up to a value of F in the former circumstance, and a particle excitation limited by the B value in the latter. First, \bar{u}_p and \bar{u}_h increase nearly as E/n at the lowest excitations, the slightly larger values for holes arising from the fact that $f_K^+(p, h, E, F)$ is smaller than $f_K(p, h, E, F)$. Next, the constrained average excitation energy of either holes (in the general case) or particles (for bound states) becomes rather

saturated at energies E above the values of F and B , respectively. The ESM basis of Eqs. (21) determines the saturation values around $F/2$ for \bar{u}_h in the former case, and around $B/2$ for \bar{u}_p in the latter. Moreover, in the limit of the $1p1h$ configuration a quite sudden change can be observed at total excitation energies around the values of F and B , respectively. There is also a small change in the trend of \bar{u}_h and \bar{u}_p just below the maximum excitation energy E for a given p - h bound-state configuration, due to the final occupation of the highest allowed single-particle levels.

To underscore the correlation between the specific shapes of the correction functions f_K , average excitation energies \bar{u}_p and \bar{u}_h , and corresponding average values of the s.p.l. densities

$$g_p(p, h) = g(F + \bar{u}_p) \quad (23a)$$

$$g_h(p, h) = g(F - \bar{u}_h), \quad (23b)$$

these quantities are shown together in Fig. 4 for the configuration $2p1h$. First, the effect of the Pauli and pairing correction is rather small. The saturations of \bar{u}_p and \bar{u}_h are distinctly caused by the bound-state condition, Fig. 4(c), and finite-depth correction, Fig. 4(d), respectively. This is why the energy dependence of $g_p(p, h)$, Fig. 4(e), is distinct from the one of $g_h(p, h)$, Fig. 4(f), either in the general case (solid curves) or for the particle-hole bound states (dotted-dashed curves).

C. ESM formula with average energy-dependent s.p.l. densities

The average energy-dependent formula was finally obtained by using the average s.p.l. densities (23) within the PSD formula (18) which becomes

$$\omega(p, h, E) = \frac{[g_p(p, h)]^p [g_h(p, h)]^h E^{n-1}}{p! h! (n-1)!} f_K(p, h, E, F). \quad (24)$$

It approximately takes into account the energy dependence of the s.p.l. density, even though the simple ESM form is still in use. However, there is no basic argument why this procedure should be used so that its accuracy needs further study.

The method adopted in this respect consists in a comparison of the results obtained by means of the approximate formula and the recursive Eq. (17). The corresponding predictions and their ratio are shown in Fig. 5 for the same simple p - h configurations. The global values $F=38$ MeV, $B=10$ MeV, $g_0=14$ MeV $^{-1}$, and $\Delta_0=1$ MeV were used. First of all, in the general case of the particle-hole state densities (i.e., for $B \rightarrow \infty$) there is only a small difference between the two PSD formulas even at medium energies. The agreement improves for more complex configurations, where the average of the single-particle excitation energies becomes really meaningful. Similar agreement is seen when the respective densities for the particle-hole bound states are compared within the first half of the energy range for each p - h configuration. However, the difference becomes significant near the maximum energy for a given particle-hole state, and increases as the PSD values drop back to zero. Nevertheless, the disagreement of these bound-state density formulas at the high-energy extremity should have little or no effect on the reaction cross-section calculations.

Therefore we may conclude that the results obtained by using the average energy-dependent s.p.l. densities within the ESM formula are rather close to the exact convolution of the energy-dependent s.p.l. density. The next question concerns the need for this average energy-dependent approach. The answer can be obtained by comparing the average energy-dependent ESM results with the PSDs given by the widely used ESM formula [36]. This is shown in Fig. 6, where the above global parameters were used. The pairing effect is apparent within this latter comparison, especially at lower energies. Besides this aspect, the behavior shown at medium energy is similar to the comparison of the recursive and Obložinský formulas in Fig. 1. The overall difference obviously exceeds the variation between the predictions of the PSD recursive formula and the average energy-dependent ESM formalism. It is rather small for the general case of the particle-hole states, Figs. 6(a) and 6(c), but larger for the bound states, Figs. 6(b) and 6(d). This strong effect following the consideration of the energy-dependent s.p.l. density is particularly caused by the constant increase in hole excitation for larger E , and the related significant decrease of the hole-state density as shown in Fig. 4(f).

D. Effect of exact Pauli-correction calculation

The Pauli-exclusion effect on particle-hole state densities has already been subject to additional investigation by Zhang and Yang [43] who used an exact method. Kalbach established later [12] that no conflict exists between their results and the frequently used Williams formulas if the energy-dependent Pauli term included pairing and passive-hole effects. The ESM derivation of PSD formulas without any approximation in the Pauli correction term was performed by Baguer *et al.* [44] and Mao Ming De and Guo Hua [13]. The latter extended the method to the case of the finite-depth potential and bound states, and included the Kalbach [12] pairing correction. The effect of the alternative use of the approximate and exact Pauli-correction, and the one caused by the average energy-dependent ESM formula are compared below.

The results that were obtained by means of Eq. (18) and according to the exact Pauli-correction formalism [13] are shown together in Fig. 7, for the most sensitive low-energy region. The analysis was first carried out without pairing correction, i.e., for $\Delta_0=0$ as shown in Figs. 7(a) and 7(c). The global value $g_0=14 \text{ MeV}^{-1}$ adopted by Fu and Kalbach [11,12] was used. Then, the PSD calculation with pairing correction corresponding to the value $\Delta_0=1 \text{ MeV}$, Figs. 7(b) and 7(d), completed the analysis of these effects under any circumstances.

The ratio of the PSD obtained by using the two formalisms, Figs. 7(c) and 7(d), shows more exactly that a close agreement – even within 1 % – is established just above the threshold for each p - h configuration. Minor deviations exist only for larger number of excitons, of less interest for multistep reaction calculations which include them in the so-called r -stage [2]. Therefore, the results of the exact Pauli-blocking effect calculations are closely related to those obtained by using the approximate Pauli correction [5,35,36]. The inclusion of a suitable pairing correction seems more significant with the following additional remark. The PSD for the very-few-exciton configurations become rather saturated within a short energy range above the threshold. On the other hand, these configurations have the main role

in the description of multistep reactions. Thus, the adequate account of the pairing effect may be found unessential for some analyses. The analysis of the high-energy limit of the particle-emission spectra, however, is quite sensitive to both pairing and nuclear-shell effects (e.g., [32,34,45]).

Finally, the comparative analysis of the effects illustrated in Figs. 6 and 7 shows, on a common basis, the higher importance of the s.p.l.-density energy dependence versus the exact calculation of the Pauli correction.

IV. REALISTIC AND GLOBAL RESULTS

The importance of the various approximations involved in the derivation of the PSD formulas should be well known in order to avoid useless effort or deficient results. First, one might want to know the consequences of the present analysis on the total state densities obtained as the sum of all PSD for allowed particle-hole numbers $p=h$. Next, one might question the usefulness of the PSD formulas discussed above, while quantum-mechanical calculations concentrating on the continuum region are being developed [30,31].

A. Effect on total state density

Average s.p. excitation energies are shown in Fig. 8 for representative $p-h$ configurations of the PSDs sum defining the total state density $\omega(E)$. The same global values $g_0=14$ MeV⁻¹, $F=38$ MeV and $\Delta_0=1$ MeV were used as above. Thus, it becomes apparent that all significant terms of this sum are characterized by rather equal \bar{u}_p and \bar{u}_h increasing nearly as E/n . The saturated average excitation energy of the holes plays a major role in the case of the few-exciton states which are vital for PE description, but not for configurations around the most probable exciton number \bar{n} [46]. The latter class of configurations mainly determine the total state density value, so that the corresponding ESM predictions are meaningful in this respect. Nevertheless, the average energy-dependent approach should be considered for the calculation of the PSD involved in the first stages of the multistep processes.

B. Consideration of the continuum effect

Shlomo [30] performed an exact quantum mechanical calculation of the s.p.l. density as the sum of the bound and continuum contributions in the case of finite potential wells. A distinct point of this approach has been the consideration of the free-gas states counted by the s.p.l. density for a finite potential well. The density of these states was calculated and subtracted by using Green's functions associated with the respective single-particle Hamiltonians. Then, the commonly used semiclassical approximations for the s.p.l. density were similarly considered for some widely used mean-field potentials. Thus, Shlomo found by means of both classes of methods that, for a realistic finite depth well, the s.p.l. density decreases with energy in the continuum region (*the continuum effect*).

This effect may have a twofold meaning for the multistep reaction calculations. First, the continuum s.p.l. density following the subtraction of the free-gas contribution should be added to the particle-hole bound state density. The latter quantity has been used for the description of the multistep compound (MSC) processes [47]. It has been assumed to be zero outside the nuclear well, which is now considered less appropriate [27]. Second, in the opinion of Bogila *et al.* [28] the subtraction of the free gas spectrum should be involved in all PSD for PE calculations. This point could be most important in accounting for the multistep direct (MSD) processes [47] which currently take into account all particle-hole states. Thus a correct yet simple method to estimate the s.p.l. density including the continuum effect is needed.

The continuum effect can be taken into account within the average energy-dependent ESM formula (24) by using a form similar to Eq. (30) of Ref. [31] (see the Appendix) for the excited-particle level density. According to Eq. (23a) it becomes

$$g_p(p, h) = \frac{3A}{2F} \left[\left(1 + \frac{\bar{u}_p}{F} \right)^{1/2} - \left(\frac{\bar{u}_p - B}{F} \right)^{1/2} \theta(\bar{u}_p - B) \right]. \quad (25)$$

To emphasize the origin of the particular behaviour of $g_p(p, h)$, this is shown at the same time as the corresponding \bar{u}_p for the basic $2p1h$ configuration in Figs. 9(b) and 9(d). It is

obvious that the average excitation energy is unchanged (see Fig. 4) so that the continuum effect fully determines the corrected s.p.l. density for excited particles. The comparison with the similar quantities \bar{u}_h and $g_h(p, h)$ (the same as in Fig. 4) demonstrates the importance of this effect, the average s.p.l. density becoming even lower for excited particles than for holes.

On the other hand, it seems worth comparing the specific average excitation energies and s.p.l. densities which determine the PSDs including the continuum effect [Figs. 9(b) and 9(d)], with the related quantities for the particle-hole bound states [Figs. 9(a) and 9(c)]. The reasons for deviations from the PSD general trend, for the two main additional classes of particle-hole state densities with variant characteristics are outlined in this way. Thus, the average excitation energies, limited by the value B for the excited particles, entirely determine the s.p.l. densities for the particle-hole bound state densities. Actually one may note that g_p has a rather constant value in this case. The value of g_h is similarly constant but obviously lower in the latter case, i.e. of the bound and continuum state density including the continuum effect. However, the above-discussed aspect of g_p is the key quantity for the second class of modified PSDs.

Moreover, these two classes of PSDs with various restrictions [Figs. 10(a) and 10(b)] are at the same time compared with the predictions of Eqs. (23) and (24) including only the finite-depth correction, also shown in Fig. 10(b). A few configurations significant in PE calculations are used in this respect. The ratios of each of the two variant PSDs to the general PSD values given in Fig. 10(b) are further shown in Figs. 10(c) and 10(d). It follows that at medium energies the size of the continuum effect on the PSD values, which is given by the latter class of ratios, is rather similar to that for the bound-state condition. Therefore, a possible replacement within MSC calculations of the particle-hole bound state density by the PSD corrected for the continuum effect [27] would not be trivial. A similar point may concern the use within the MSD calculations of the PSD either including the continuum effect [28] or taking into account the free-gas single particle levels as well.

The relation between the results of Eq. (25) and the quantum-mechanical (QM) calcu-

lations should be also considered before further use of the former in reaction calculations. Hence, following Shlomo *et al.* [30,31], the s.p.l. density was calculated [48] by using the respective relation with Green's function. As an alternative to the smearing procedure, the imaginary part of Green's function has been calculated separately for the discrete and continuous states. The regular and Jost solutions of the radial Schrödinger equation are used in the continuum. The smooth part of the rapidly fluctuating s.p.l. density is calculated by means of the Strutinski smoothing procedure [49]. The Woods-Saxon (WS) potential [30] was considered in this frame as well as in the semiclassical Thomas-Fermi (TF) formula, with the similar results shown in Fig. 11(a). The familiar FGM shape is given by the TF formula with an infinite square-well (SQ) potential, while the corresponding finite well (FSQ) illustrates the continuum effect in Fig. 11(b). It should be noted that the continuum component of the s.p.l. density is nearly the same within either exact quantum-mechanical calculations with the WS potential, or TF approximation with either the WS or the FSQ potential wells, provided that the free-gas contribution is subtracted. Moreover, a similar trend is obtained by means of the simple FGM formula (25) taking into account the continuum effect. Nevertheless, the quantum-mechanical s.p.l. density can be related to this formula only for a reduced Fermi energy, e.g. $\bar{F} \simeq 20$ MeV [50]. This value has been obtained as an average value along the trajectory of the incident projectile with respect to the both nuclear density and first nucleon-nucleon collision probability. The usual value $F=38$ MeV causes lower $g(\varepsilon_F)$ values, that are not consistent with the phenomenological data.

Therefore one may use the simple FGM energy dependence, within an appropriate form which matches the quantum-mechanical s.p.l. density including the continuum effect, in the average energy-dependent ESM formalism. This unsophisticated yet improved method could provide the correct PSDs for MSD/MSD calculations, in agreement with the consideration that the highly-excited single-particle states are not strongly coupled to compound nuclear states [51] or partially relaxed states of composite nuclei formed in nuclear reactions at intermediate energies [52,53]. The question is additionally made intricate by the recent proof of a much shorter time scale required to reach thermal equilibration in intermediate-

energy nucleon-induced reactions, found to be of the order of $\sim 10^{-22}$ sec [54]. Further experimental-data analyses should thus consider a combination of reaction models and related PSD formalisms as well.

V. SUMMARY AND CONCLUSIONS

The particle-hole state density has been obtained by means of recursive relations, for the bound as well as bound-plus-continuum states. The corresponding expressions, i.e., Eqs. (9) and (17), can be used for various energy dependences of the excited-particle and hole state densities while the particular case of the FGM is discussed. We have underlined that consideration of the finite depth of the nuclear-potential well should be explicitly present in the particle-hole state density formulas exceeding the ESM framework.

Next, the results of the recursive formula are compared with the Kalbach [18] approximation still within the ESM formula but using distinct average s.p.l. densities for the holes and excited particles respectively, at their average excitation energies. At the same time the Kalbach formalism is extended to the case of the bound states, while the pairing and Pauli-blocking effects have been included in all terms of the ESM correction function. The correctness of the average energy-dependent ESM approach is established by reference to the rigorous convolution (9) of the energy-dependent s.p.l. densities for the case of the FGM dependence. The difference between the predictions of the two methods is compared with the similar variation between average energy-dependent form and the standard formula [35,36], the former being much lower especially in the bound-state case.

The exact calculation of the Pauli-blocking effect, which is close to the well-known approximate Pauli correction [5,35,36], is also discussed. Thus it is shown on a common basis the higher importance of the s.p.l.-density energy dependence versus the exact calculation of the Pauli correction. The significant role of the pairing correction is pointed out, while comments are made on the circumstances under which the adequate account of the pairing effects could indeed appear less than essential [45].

The continuum effect has been considered for the case of a FGM energy dependence in the average energy-dependent ESM approach. The continuum component of the s.p.l. density is found rather similar using either exact quantum-mechanical calculations with the Woods-Saxon potential, or Thomas-Fermi approximation with WS as well as finite-square potential wells, provided that the free-gas contribution is subtracted. A similar trend is obtained by means of the simple FGM formula for the s.p.l. density if the continuum effect is taken into account. It should be noted that no arbitrary truncation, e.g. in the range 15-25 MeV [38], is thus necessary in order to take care for the continuum effect within the s.p.l. density account. On the other hand, since the actual quantum-statistical analyses of the multistep reactions use the rough ESM, the results following consideration of the effective NN -interaction strength as the only free parameter could be altered. This point is the subject of current work along with systematic calculations of the s.p.l. density in the continuum and the correlation with PE surface effects [18,50].

ACKNOWLEDGMENTS

The authors are grateful to Marshall Blann, Emil Betak, Zhang Jingshang, and Shalom Shlomo for valuable discussions. Thanks are also due to the referees of this work for helpful critiquing. Assistance of Ms. Vivien Prager with improving the manuscript is acknowledged. This work has been carried out under the Romanian Ministry of Research and Technology Contract No. 4/A13 and the Research Contract No. 8886/R1 of the International Atomic Energy Agency (Vienna).

APPENDIX: FERMI GAS MODEL S.P.L. DENSITY IN CONTINUUM

The s.p.l. density associated with a local mean field V has the following expression in the Thomas-Fermi approximation, by taking into account the spin degeneracy and neglecting the spin-orbit interactions [28,30,55]

$$g^{TF}(\epsilon) = \frac{1}{2\pi^2} \left(\frac{2m}{\hbar^2} \right)^{3/2} \int d\mathbf{r} (\epsilon - V(\mathbf{r}))^{1/2} \Theta(\epsilon - V(\mathbf{r})). \quad (\text{A1})$$

The single-particle energy ϵ is measured relative to the top of the nuclear well, in order to make a clear distinction between the bound states at $\epsilon \leq 0$ and unbound continuum states at $\epsilon > 0$.

For the finite well potentials, the nucleus can be imagined inside a spherical box of radius R larger than the range of $V(r)$ (see Fig. 1 of [29]). In the case of a square potential well of radius R_0 and depth $V_0 < 0$, we have from Eq. (A1)

$$g_{\Omega}^{TF}(\epsilon) = \frac{1}{2\pi^2} \left(\frac{2m}{\hbar^2} \right)^{3/2} \left[\Omega_0(\epsilon - V_0)^{1/2} \Theta(\epsilon - V_0) + \Omega \epsilon^{1/2} \Theta(\epsilon) - \Omega_0 \epsilon^{1/2} \Theta(\epsilon) \right], \quad (\text{A2})$$

where $\Omega_0 = 4\pi R_0^3/3$ and $\Omega = 4\pi R^3/3$. Since the properties of the nucleus itself do not depend on R [29], in the case of the finite square well one has to subtract the contribution of free Fermi gas when $\epsilon > 0$ [28,30,31]

$$g_f(\epsilon) = \frac{\Omega}{2\pi^2} \left(\frac{2m}{\hbar^2} \right)^{3/2} \epsilon^{1/2}. \quad (\text{A3})$$

The s.p.l. density which is thus obtained

$$g_{FSQ}^{TF}(\epsilon) = \frac{1}{2\pi^2} \left(\frac{2m}{\hbar^2} \right)^{3/2} \Omega_0 \left[(\epsilon - V_0)^{1/2} \Theta(\epsilon - V_0) - \epsilon^{1/2} \Theta(\epsilon) \right], \quad (\text{A4})$$

has the well-known FGM form except the continuum correction term. In terms of the single-particle energy $\varepsilon = \epsilon - V_0$ which is measured relative to the bottom of the nuclear well, it becomes

$$g_{FSQ}^{TF}(\varepsilon) = g_0 \left[\left(\frac{\varepsilon}{F} \right)^{1/2} - \left(\frac{\varepsilon + V_0}{F} \right)^{1/2} \Theta(\varepsilon + V_0) \right], \quad (\text{A5})$$

where $g_0 = g(\epsilon_F) = g(F)$ with reference to both notations used for the s.p.l. energy. Actually, the derivation of Eq. (A4) shows that the radius R is indeed taken into account but $g_{FSQ}^{TF}(\epsilon)$ does not depend on it. Therefore, the final expression is apparently only a difference of terms calculated for the SQ potential well and the free-particle case, respectively, within an infinite spherical box with the radius R_0 .

REFERENCES

- [1] E. Gadioli and P.E. Hodgson, *Pre-Equilibrium Nuclear Reactions* (Oxford University Press, Oxford, 1992).
- [2] H. Feshbach, *Theoretical Nuclear Physics: Nuclear Reactions* (Wiley, New York, 1992).
- [3] T. Ericson, *Adv. in Phys.* **9**, 425 (1960).
- [4] A. Bohr and B.R. Mottelson, *Nuclear Structure* (W.A. Benjamin, Inc., Advanced Book Program, Reading, 1969), p. 153.
- [5] F.C. Williams, *Nucl. Phys.* **A166**, 231 (1971).
- [6] M. Herman, G. Reffo, M. Rosetti, G. Giardina, and A. Italiano, *Phys. Rev. C* **40**, 2870 (1989).
- [7] M.B. Chadwick and G. Reffo, *Phys. Rev. C* **44**, 919 (1991); M.B. Chadwick, P. Obložinský, P.E. Hodgson, and G. Reffo, *ibid.* **44**, 814 (1991).
- [8] F.C. Williams, Jr., A. Mignerey, and M. Blann, *Nucl. Phys.* **A207**, 619 (1973); K. Albrecht and M. Blann, *Phys. Rev. C* **8**, 1481 (1973); W. Scobel *et al.*, *ibid.* **30**, 1480 (1984).
- [9] M. Blann and G. Reffo, in International Atomic Energy Agency Report No. INDC(NDS) - 214/LJ, Vienna, 1989, p. 75.
- [10] G. Reffo and M. Herman, in *Proceedings of the International Conference on Nuclear Data for Science and Technology, Gatlinburg, Tennessee, 1994*, edited by J.K. Dickens (American Nuclear Society, 1994), p. 473; M. Herman, G. Reffo, H. Lenske, and H. Wolter, *ibid.*, p. 466.
- [11] C.Y. Fu, *Nucl. Sci. Eng.* **86**, 344 (1984).
- [12] C. Kalbach, *Nucl. Sci. Eng.* **95**, 70 (1987); *Z. Phys. A* **332**, 157 (1989).

- [13] Mao Ming De and Guo Hua, J. Phys. G **19**, 421 (1993).
- [14] M. Blann, Phys. Rev. Lett. **28**, 757 (1972); Nucl. Phys. **A213**, 570 (1973); in *Proceedings of the International School of Nuclear Physics, Predeal, Romania, 1974*, edited by A. Ciocanel (Editura Academiei, Bucharest, 1974), p. 249; see also Phys. Rev. C **54**, 1341 (1996).
- [15] E. Gadioli, E. Gadioli Erba, and P.G. Sona, Nucl. Phys. **A217**, 589 (1973).
- [16] E. Gadioli, E. Gadioli Erba, and J.J. Hogan, Phys. Rev. C **16**, 1404 (1977).
- [17] C. Kalbach, Phys. Rev. C **23**, 124 (1981).
- [18] C. Kalbach, Phys. Rev. C **32**, 1157 (1985).
- [19] M.B. Chadwick and P. Obložinský, Phys. Rev. C **44**, R1740 (1991); **46**, 2028 (1992).
- [20] J.S. Zhang and S.G. Wu, Chinese J. Nucl. Phys. **14**, 121 (1992).
- [21] Ye.A. Bogila, V.M. Kolomietz, and A.I. Sanzhur, Z. Phys. A **341**, 373 (1992).
- [22] G. Ghosh, R.W. Hasse, P. Schuck, and J. Winter, Phys. Rev. Lett. **50**, 1250 (1983).
- [23] A.H. Blin, B. Hiller, R.W. Hasse, and P. Schuck, J. de Phys. **45**, C6-231 (1984).
- [24] R.W. Hasse and P. Schuck, Nucl. Phys. **A445**, 205 (1985).
- [25] P. Schuck, R.W. Hasse, J. Jaenicke, C. Grigoire, B. Remaud, F. Sebillé, and E. Suraud, in *Progress in Particle and Nuclear Physics* (Pergamon Press, Oxford, 1989), vol. 22, p. 181.
- [26] K. Sato and S. Yoshida, Phys. Rev. C **49**, 1099 (1994); M. Abe, S. Yoshida, and K. Sato, Phys. Rev. C **52**, 837 (1995).
- [27] S. Shlomo, Ye.A. Bogila, V.M. Kolomietz, and A.I. Sanzhur, Z. Phys. A **353**, 27 (1995).
- [28] Ye.A. Bogila, V.M. Kolomietz, A.I. Sanzhur, and S. Shlomo, Phys. Rev. C **53**, 855

- (1996).
- [29] D.R. Dean and U. Mosel, *Z. Phys. A* **322**, 647 (1985).
- [30] S. Shlomo, *Nucl. Phys.* **A539**, 17 (1992).
- [31] S. Shlomo, V.M. Kolomietz, and H. Dejbakhsh, *Phys. Rev. C* **55**, 1972 (1997).
- [32] M. Avrigeanu and V. Avrigeanu, *J. Phys. G* **20**, 613 (1994).
- [33] M. Avrigeanu, A. Harangozo, and V. Avrigeanu, in *Proc. of the 7th Int. Conf. on Nuclear Reaction Mechanisms, Varenna, 1994*, edited by E. Gadioli (Ricerca Scientifica ed Educazione Permanente, Milano, 1994), p. 165.
- [34] M. Avrigeanu, A. Harangozo, and V. Avrigeanu, IPNE-Bucharest Report NP-85-1995; *Rom. J. Phys.* **41**, 77 (1996).
- [35] E. Běták and J. Dobeš, *Z. Phys. A* **279**, 319 (1976).
- [36] P. Obložinský, *Nucl. Phys.* **A453**, 127 (1986).
- [37] D.L. Tubbs and S.E. Koonin, *Astrophys. J.* **232**, L59 (1979).
- [38] T.J. Mazurek, J.M. Lattimer, and G.E. Brown, *Astrophys. J.* **229**, 713 (1979).
- [39] M. Herman, G. Reffo, and C. Costa, *Phys. Rev. C* **39**, 1269 (1989).
- [40] K.-H. Schmidt, H. Delagrange, J.P. Dufour, N. Cârjan, and A. Fleury, *Z. Phys. A* **308**, 215 (1982).
- [41] J.-J. Gaimard and K.-H. Schmidt, *Nucl. Phys.* **A531**, 709 (1991).
- [42] W. Dilg, W. Schantl, H. Vonach, and M. Uhl, *Nucl. Phys.* **A217**, 269 (1973).
- [43] J.S. Zhang and X.L. Yang, *Z. Phys. A* **329**, 69 (1988).
- [44] N. Baguer, R. Capote, and R. Pedrosa, *Z. Phys. A* **334**, 397 (1989).
- [45] Y. Watanabe, A. Aoto, H. Kashimoto, S. Chiba, T. Fukahori, K. Hasegawa, M. Mizu-

- moto, S. Meigo, M. Sugimoto, Y. Yamanouti, N. Koori, M.B. Chadwick, and P.E. Hodgson, Phys. Rev. C **51**, 1891 (1995).
- [46] C.Y. Fu, Nucl. Sci. Eng. **92**, 440 (1986).
- [47] H. Feshbach, A. Kerman, and S. Koonin, Ann. Phys. (N.Y.) **125**, 429 (1980).
- [48] I. Şteţcu, report nucl-th/9711007; Rom. J. Phys. (in press).
- [49] C.K. Ross and R.K. Bhaduri, Nucl. Phys. **A188**, 566 (1972).
- [50] M. Avrigeanu, A. Harangozo, V. Avrigeanu, and A.N. Antonov, Phys. Rev. C **54**, 2538 (1996).
- [51] S.M. Grimes, Phys. Rev. C **42**, 2744 (1990).
- [52] H.A. Weidenmüller, Phys. Lett. **10**, 331 (1964).
- [53] M.G. Mustafa, M. Blann, A.V. Ignatyuk, and S.M. Grimes, Phys. Rev. C **45**, 1078 (1992); M.G. Mustafa, M. Blann, and A.V. Ignatyuk, *ibid.* **48**, 588 (1993).
- [54] S. Chiba, K. Niita, and O. Iwamoto, Phys. Rev. C **54**, 3302 (1996).
- [55] P. Ring and P. Schuck, *The Nuclear Many-Body Problem* (Springer, Berlin, 1980), Ch. 13.

FIGURE CAPTIONS

- FIG. 1. The convolution state density given by Eq. (9), divided by the Obložinský formula without Pauli correction (solid curves), as well as by the Ericson formula (dashed curves), for the given p - h configurations. In Eq. (9) and the Obložinský formula, $F=38$ MeV and the limit of large B is considered. For all calculations $g_0=14$ MeV⁻¹.
- FIG. 2. The correction function for the Pauli blocking, nuclear-potential finite depth and pairing-correlation effects, of the ESM particle-hole state density for given p - h configurations. The calculations use the finite-depth correction alone with $F=38$ MeV (dotted curves), the Pauli correction without (dashed curves) and with the pairing effects included (solid curves), and also the bound-state condition with $B=10$ MeV (dash-dotted curves).
- FIG. 3. (a),(b) The $f_K^+(p, h, E, F)$ and (c),(d) the $f_K(p, h, E, F)$ correction functions to the ESM formula for the Pauli blocking, potential finite-depth and pairing-correlation effects, as well as (e),(f) the average excitation energies for particles and holes within the given p - h configurations, for (a),(c),(e) the particle-hole bound plus continuum states, and (b),(d),(f) the bound states only. For all calculations $F=38$ MeV, and $B=10$ MeV is considered for the bound states.
- FIG. 4. (a) The $f_K^+(p, h, E, F)$ and (b) $f_K(p, h, E, F)$ correction functions to the ESM formula for the Pauli blocking, potential finite-depth and pairing-correlation effects, (c),(d) the average excitation energies for particles and holes, and (e),(f) the average energy-dependent s.p.l. densities for excited particles and holes, for the $2p1h$ configuration. The meaning of the curves is the same as in Fig. 2 except that the dotted line in (e) and (f) gives the value of g_0 . For all calculations $g_0=14$ MeV⁻¹ and $F=38$ MeV, while $B=10$ MeV is considered for the bound states.
- FIG. 5. The particle-hole state densities for the given p - h configurations, obtained with the average energy-dependent ESM formalism (solid curves) and the PSD recursive formula (dashed curves), and their ratio, for (a),(c) bound-plus-continuum states, and (b),(d)

bound states only. The same global values are used as in Fig. 4.

- FIG. 6. The same as Fig. 5 except the latter PSD formula considered in the comparison is the ESM formula [36] (dash-dotted curves).
- FIG. 7. (a),(b) The particle-hole state densities for given n -exciton configurations with $p=h$, obtained with the ESM formulas including the advanced pairing correction [12] and either the exact correction for the Pauli exclusion principle [13] (solid curves) or the respective approximate form [36] (dashed curves), and (c),(d) their ratios. For all calculations $g_0=14 \text{ MeV}^{-1}$, while $\Delta_0=1 \text{ MeV}$ is considered for the pairing correction account in (c) and (d).
- FIG. 8. Average excitation energies of the excited particles (dotted curves) and holes (dashed curves) for given n -exciton configurations with $p=h$, as function of the total excitation energy. The same global values are used as in Fig. 4, while $\Delta_0=1 \text{ MeV}$ is considered for the pairing correction account.
- FIG. 9. (a),(b) The average excitation energies and (c),(d) the related s.p.l. densities for (a),(c) the particle-hole bound states, and (b),(d) the general case including (solid curves) or not (dotted curve) the continuum effect, for the $2p1h$ configuration. The same global values are used as in Fig. 4.
- FIG. 10. The particle-hole state densities for the given $p-h$ configurations, obtained within the average energy-dependent ESM formalism for (a) the bound states and (b) the bound-plus-continuum states including the continuum effect (solid curves) or taking into account also the free-gas single particle levels as given by Eqs. (23) and (24) in the limit of large B and with only the finite-depth correction (dotted curves), and (c),(d) the ratios of each of the two kinds of variant PSDs to the third one. The same global values are used as in Fig. 4.
- FIG. 11. The comparison of the smoothed quantum-mechanical s.p.l. density for the neutrons of the nucleus ^{56}Fe (solid curve) and the results of the TF approximation using (a) the same Woods-Saxon potential well as within the QM calculation, and (b) the infinite (SQ) and finite square potential wells (FSQ) (dashed curves), and the FGM formula

with the Fermi-energy values of $F=38$ MeV (dotted curve) and $\bar{F}=20$ MeV (dot-dashed curve). For parameters of the potential wells see Refs. [30,48].

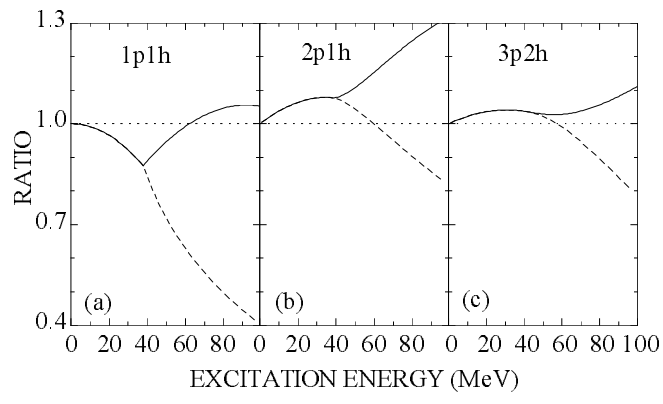


FIG. 1.

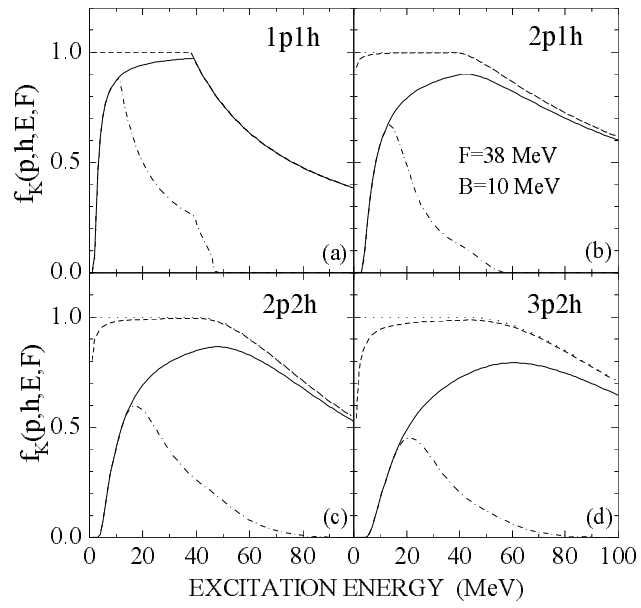


Fig. 2

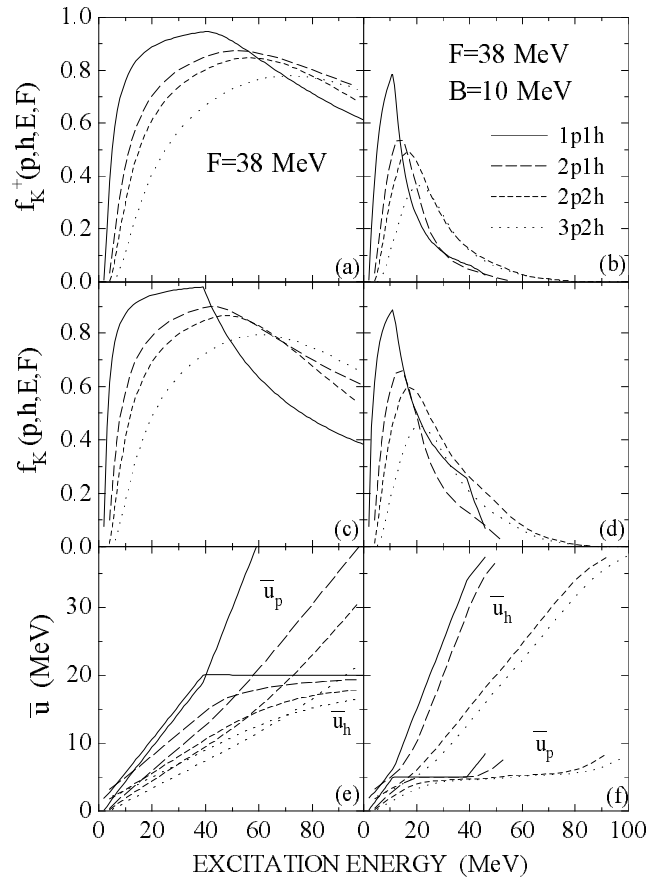


Fig. 3

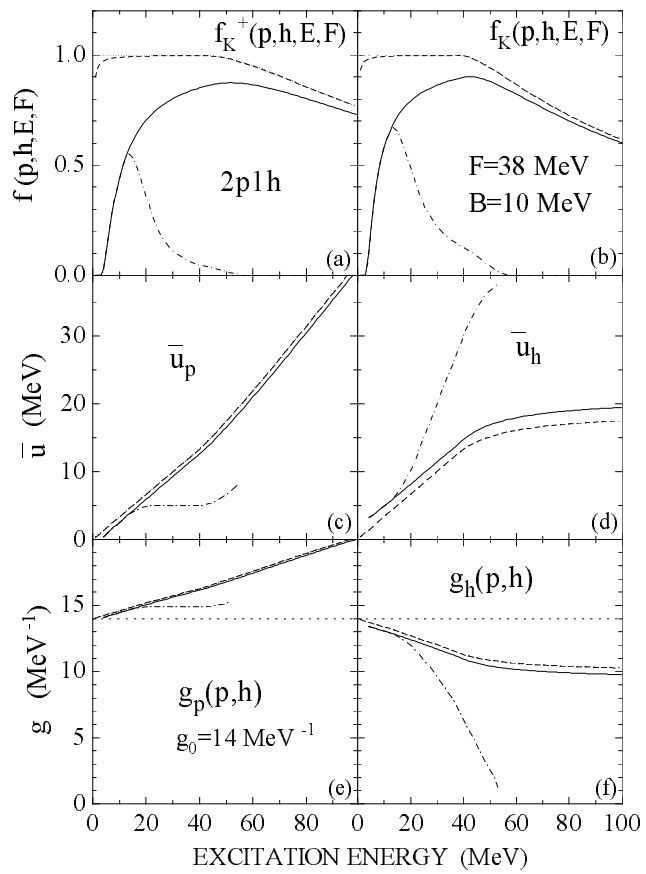


Fig. 4

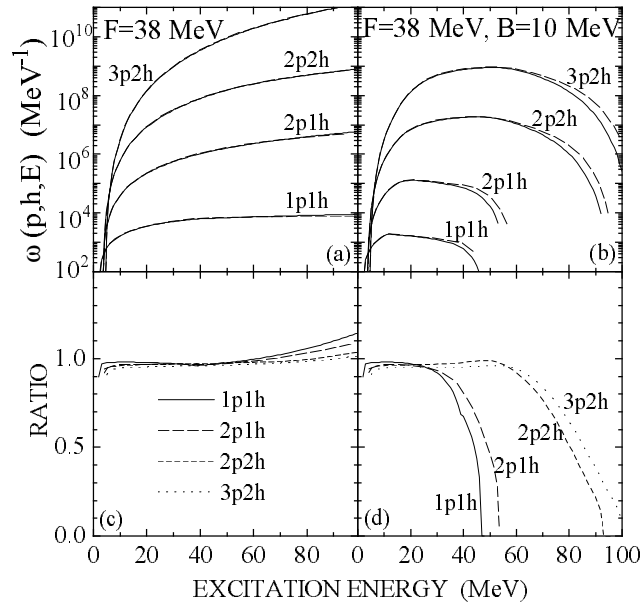


Fig. 5

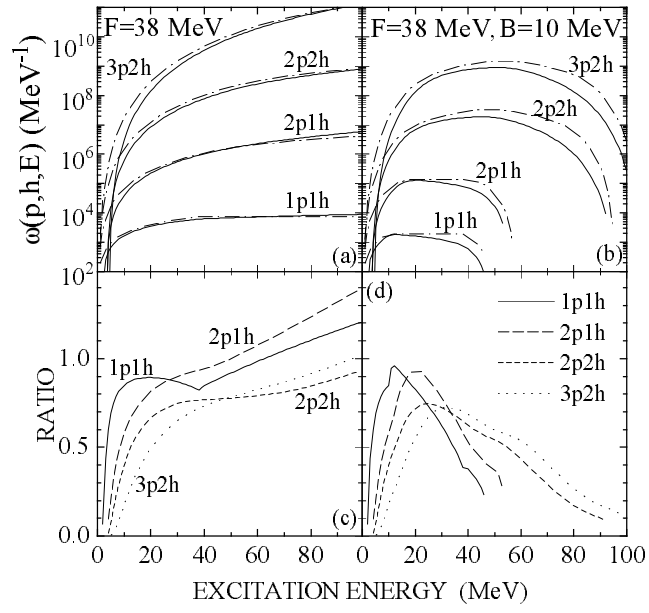


Fig. 6

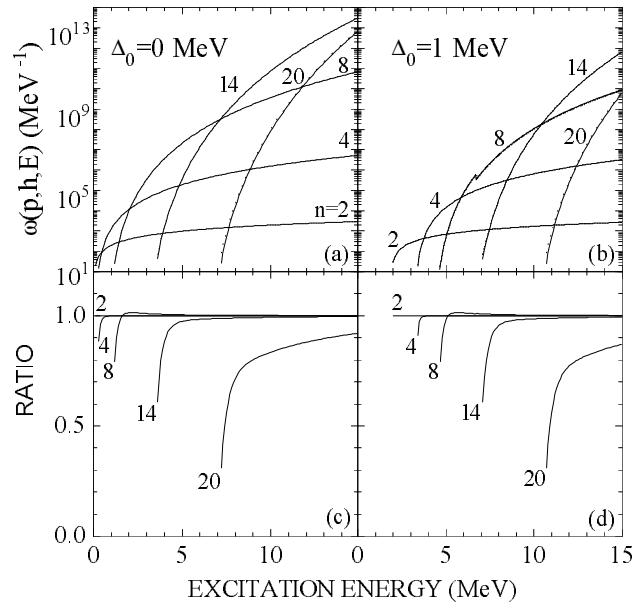


Fig. 7

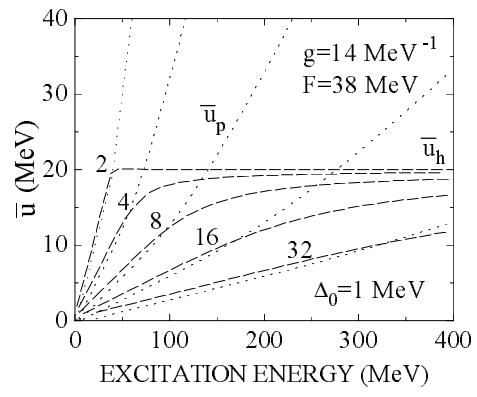


Fig. 8

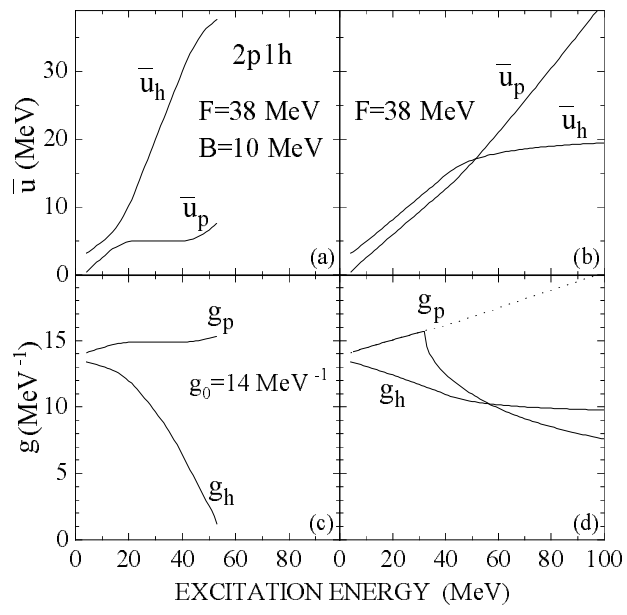


Fig. 9

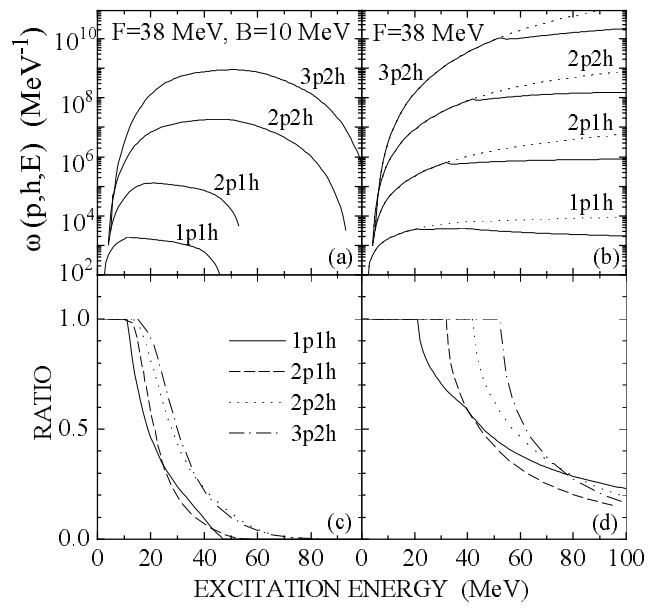


Fig. 10

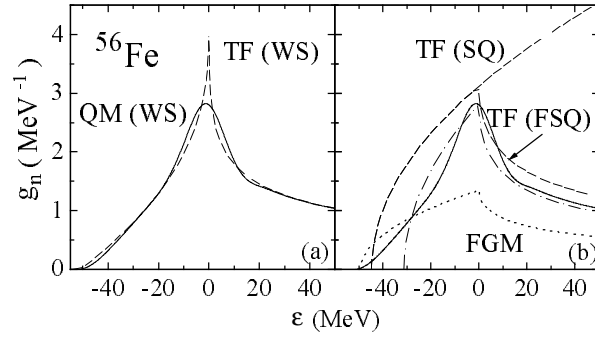


Fig. 11